Frontiers of Information Technology & Electronic Engineering
www.zju.edu.cn/jzus; engineering.cae.cn; www.springerlink.com
ISSN 2095-9184 (print); ISSN 2095-9230 (online)
E-mail: jzus@zju.edu.cn

Adaptive fuzzy integral sliding mode velocity control for the cutting system of a trench cutter*

Qi-yan TIAN, Jian-hua WEI, Jin-hui FANG†‡, Kai GUO

(*State Key Laboratory of Fluid Power & Mechatronic Systems, Zhejiang University, Hangzhou 310027, China*)

†E-mail: jhfang@zju.edu.cn

Received June 1, 2015; Revision accepted Oct. 26, 2015; Crosschecked Dec. 9, 2015

Abstract: This paper presents a velocity controller for the cutting system of a trench cutter (TC). The cutting velocity of a cutting system is affected by the unknown load characteristics of rock and soil. In addition, geological conditions vary with time. Due to the complex load characteristics of rock and soil, the cutting load torque of a cutter is related to the geological conditions and the feeding velocity of the cutter. Moreover, a cutter's dynamic model is subjected to uncertainties with unknown effects on its function. In this study, to deal with the particular characteristics of a cutting system, a novel adaptive fuzzy integral sliding mode control (AFISMC) is designed for controlling cutting velocity. The model combines the robust characteristics of an integral sliding mode controller with the adaptive adjusting characteristics of an adaptive fuzzy controller. The AFISMC cutting velocity controller is synthesized using the backstepping technique. The stability of the whole system including the fuzzy inference system, integral sliding mode controller, and the cutting system is proven using the Lyapunov theory. Experiments have been conducted on a TC test bench with the AFISMC under different operating conditions. The experimental results demonstrate that the proposed AFISMC cutting velocity controller gives a superior and robust velocity tracking performance.

Key words: Cutting system, Electro-hydraulic system, Cutting velocity control, Adaptive fuzzy integral sliding mode control
http://dx.doi.org/10.1631/FITEE.15a0160 **CLC number:** TP271.3

1 Introduction

The development of the diaphragm walling technique and the introduction of trench cutter technology have changed civil engineering significantly. The trench cutter (TC) is now the most advanced construction machinery used for diaphragm walling. A system driven by hydraulic motors provides a cutting motion and breaks rock, making it a critical part of trench cutting. Controlling the cutting velocity of a TC is of great importance in the operating process to ensure construction efficiency and safety, but it is affected by unknown load characteristics and varying geological conditions, making velocity control intricate a very complicated problem. In addition, fast dynamic response and high energy efficiency are both desirable in a TC cutting velocity control system. Valve-controlled systems can achieve a fast dynamic response and high system accuracy, but the system efficiency is comparatively low and sometimes even unacceptable (Chiang *et al.*, 2004). Pump-controlled systems can effectively eliminate the energy consumption due to throttling losses and have the potential to obtain good dynamic performance (Wu and Lee, 1995; Minav *et al.*, 2013).

To improve the dynamic performance of pump-controlled systems, various control algorithms have been designed. Daher and Ivantysynova (2013) were first to apply pump displacement control to an electro-hydraulic power steering system. Linearization control techniques were used to design a primary controller based on a simplified and linearized plant model to control the actuator force of the steering

‡ Corresponding author
* Project supported by the National High-Tech R&D Program (863) of China (No. 2012AA041801)
ORCID: Qi-yan TIAN, http://orcid.org/0000-0002-8392-7252

system. However, linear control theory is limited to a wide range of operating points and difficult nonlinearities. Therefore, nonlinear control algorithms have been designed to overcome nonlinear and parametric uncertainties associated with hydraulic systems. Wang *et al.* (2012) used singular perturbation theory and Lyapunov techniques to simplify control designs for hydraulic pump controlled systems to make the control algorithm suitable for engineering practice. Several robust controllers were also designed to achieve satisfactory performance of not only the pump-controlled systems (Ahn *et al.*, 2007; Truong and Ahn, 2011), but also systems in industrial applications (Shi *et al.*, 2013). Truong and Ahn (2009) presented a hydraulic hybrid load simulator and designed a fuzzy self-tuning PID controller to obtain robust force control performance. The H_∞ based linear quadratic regulator (LQR) control was employed to optimize the tracking controller design of discrete-time Takagi-Sugeno (T-S) fuzzy systems (Zhang *et al.*, 2013). A decoupling fuzzy sliding mode controller was proposed for the clamping force and energy saving control in a hydraulic injection moulding machine to improve control performance and energy efficiency simultaneously (Chiang *et al.*, 2005). In addition, Lin *et al.* (2013) designed a robust discrete-time sliding mode controller for an electro-hydraulic pump controlled actuator system to deal with the adverse influence of nonlinear friction on system dynamic performance. A sliding mode controller based on an improved friction model was designed to obtain better velocity tracking performance and increased robustness of a hydraulic pump-controlled elevator (Sha *et al.*, 2002). However, chattering in the control signal due to the sliding mode controller can easily excite high frequency modes and degrade the system performance (Guo *et al.*, 2015). Adaptive control was proposed to automatically adjust the controller parameters and has been widely used in the presence of parameter uncertainties. An adaptive controller was designed to control the velocity of a pump-controlled steering actuator, in which an indirect self-tuning regulator algorithm is used to estimate plant parameters (Daher and Ivantysynova, 2014). Wei *et al.* (2015) designed a nonlinear controller including a disturbance observer, a nonlinear feedforward controller, and a feedback controller to improve supply pressure tracking performance of a hydraulic pump in the presence of unknown time-varying load flow disturbances. The adaptive backstepping approach was applied to design a flow controller for U-tube steam generator whose dynamic responses varied significantly when the load changed (Wei *et al.*, 2014). Busquets and Ivantysynova (2015) proposed a nonlinear discontinuous projection-based adaptive robust controller (ARC) for precision motion control of displacement control actuators.

Most of the above studies paid attention to nonlinear and parametric uncertainties. However, due to the complex load characteristics of rock and soil, the cutting torque of a TC is dependent on geological conditions and feed velocity. Moreover, its dynamic model is subjected to uncertainties with unknown effects on its function. Without an explicit plant model, adaptive control is not suitable for controlling the cutting velocity of a cutting system. Moreover, the cutting torque cannot be measured on the actual equipment. Therefore, the actuator load torque is a significant factor affecting velocity control and may severely affect the performance of cutting velocity tracking and the robustness of a cutting system. Fuzzy logic is an intelligent control method, which behaves like humans and is independent of the plant model (Lin and Huang, 2007; Wang *et al.*, 2011). The free fuzzy control approach has been widely used in electro-hydraulic servo systems (Chen *et al.*, 2008; Kalyoncu and Haydim, 2009). However, the fuzzy rules have to be adjusted through trial and error, which is time consuming. Therefore, adaptive fuzzy control (Wang *et al.*, 2012; Cerman, 2013) has been proposed to adjust the fuzzy sets, and better control performance has been achieved.

In this paper, we propose an adaptive fuzzy integral sliding mode control (AFISMC) scheme for controlling the cutting velocity of a cutting system. The controller combines the robust characteristics of an integral sliding mode control with the adaptive adjusting characteristics of an adaptive fuzzy control. The AFISMC cutting velocity controller was synthesized using the backstepping technique. The stability of the whole system including the integral sliding mode controller, the fuzzy inference system, and the controlled plant is proven using the Lyapunov theory.

2 Architecture and mathematical model

2.1 System architecture

The cutting system of a TC is shown schematically in Fig. 1. The configuration of the cutting system, including the hydraulic cutting motor, variable displacement pump, pilot operated directional valve, safety relief valve, coupling shaft, and cutter, was achieved by integrating hydraulic components and mechanical apparatus. A variable displacement pump driven by a constant speed diesel engine is connected to a fixed displacement hydraulic motor. A pilot operated directional valve is employed to control the motor rotation direction. A safety relief valve is used to establish an upper limit to the line pressures and protect the system from damage due to pressure peaks. The displacement control of the pump is accomplished by means of a pilot servo valve with electrical feedback of the swashplate angle.

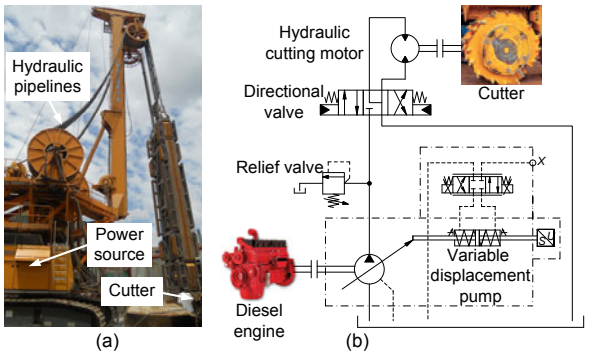

Fig. 1 Architecture of a trench cutter (TC)
(a) Photograph of a TC at a construction site; (b) A schematic diagram of a cutting system of a TC

The cutting velocity control of the cutting system is subjected to unknown load characteristics of rock or soil, and the geological conditions are time-varying. Due to the complex load characteristics of rock or soil, the cutting load torque of a cutter is related to geological conditions and the cutting and feeding velocities of the cutter. These particular characteristics of a cutting system present great challenges for cutting velocity controller design.

2.2 Mathematical model

The viscous damping and motor friction are fairly small compared with the load torque exerted on the motor and can be neglected without influencing the accuracy of the plant model. For simplicity, the torque balance equation of the cutting hydraulic motor can be written as

$$J\dot{\omega} = pD - f(\omega, v_f), \tag{1}$$

where J is the effective inertia of the motor and load, ω the rotational angular speed of the motor shaft, p the pressure at the inlet port of the hydraulic motor, D the volumetric displacement of the motor, v_f the feeding velocity of the cutter, and $f(\omega, v_f)$ the load torque acting on the hydraulic cutting motor. Due to the complex load characteristics of rock or soil, the load torque on the motor is related to geological conditions, cutting rotational velocity, and feeding velocity of the cutter, but the nonlinear functional relationships among them are unknown.

The continuity equation for the inlet chamber of a cutting motor can be written as (Merritt, 1967)

$$\dot{p} = \frac{\beta_e}{V}(k_p\alpha_p - D\omega - c_t p), \tag{2}$$

where β_e is the effective hydraulic fluid bulk modulus, V the total volume of the inlet chamber, k_p the pump flow gain, α_p the swashplate angle of the pump, and c_t the total leakage coefficient of the pump and motor.

Define the system state variables as $\boldsymbol{x}=[x_1, x_2]^T=[\omega, p]^T$. The whole system can be written as

$$\begin{cases} \dot{x}_1 = \dfrac{1}{J}[Dx_2 - f(x_1, v_f)], \\ \dot{x}_2 = \dfrac{\beta_e}{V}(k_p\alpha_p - Dx_1 - c_t x_2). \end{cases} \tag{3}$$

3 Controller design

Given the desired velocity reference $x_{1d}(t)$, the goal of the controller is to guarantee that the output can track the desired trajectory as closely as possible in the presence of unknown disturbance. Using the backstepping technique, the controller is shown as follows.

Step 1:

Define the tracking error as $\tilde{x}_1 = x_1 - x_{1d}$. Then

an integral sliding surface s_1 is defined in the following form:

$$s_1 = \tilde{x}_1 + \lambda \int \tilde{x}_1 \mathrm{d}t, \tag{4}$$

where λ is a positive constant. Since decreasing $\tilde{x}_1$ is the same as decreasing s_1, the aim is to make s_1 as small as possible. The time derivative of s_1 along the system can be written as

$$\dot{s}_1 = \dot{\tilde{x}}_1 + \lambda \tilde{x}_1 = \frac{1}{J}(Dx_2 - f) - \dot{x}_{1\mathrm{d}} + \lambda \tilde{x}_1. \tag{5}$$

However, f is an unknown nonlinear function, so the ideal control law cannot be implemented. Fuzzy control imitating human logic is independent of the plant model and therefore is well suited to this system. Here, the design of an online tuning fuzzy system through an adaptive mechanism is described.

In the fuzzy controller, a product inference engine, singleton fuzzification, and center average defuzzification are employed. The input membership functions should be at least twice continuously differentiable to use the backstepping technique. In addition, the membership function should be as simple as possible to ease implementation. Therefore, we designed a novel membership function, which is twice continuously differentiable for the two input variables (Fig. 2).

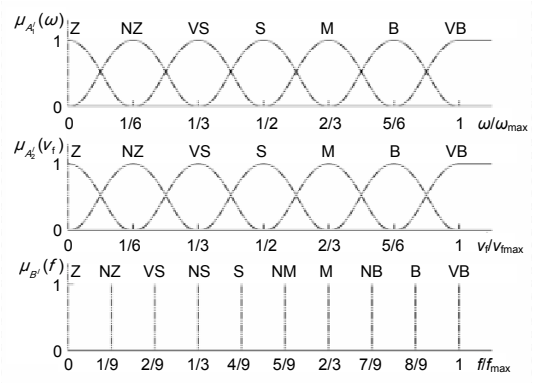

Fig. 2 Fuzzy sets and membership functions

The twice continuously differentiable function of the two input variables is expressed as follows:

$$\mu_{A_k^i}(\boldsymbol{x}) = -\frac{[(\boldsymbol{x} - c_{kj})^2 + \sigma_{kj}^2][(\boldsymbol{x} - c_{kj})^2 - \sigma_{kj}^2]^3}{\sigma_{kj}^8}, \tag{6}$$

where $\mu_{A_k^i}$ is the membership function value of the input variables, i (i=1, 2, …, m) denotes the fuzzy rule number, k (k=1, 2) denotes the input variable number, j (j=1, 2, …, n) denotes the input variable membership function number, and σ_{kj} and c_{kj} are respectively the width and center of the membership functions of the controlled cutting velocity and the cutter feeding velocity.

The rules describing the fuzzy system are shown in Table 1. The knowledge base contains a set of IF-THEN rules, in which the ith rule is shown as follows:

$R^{(i)}$: IF ω is A_1^i and v_f is A_2^i THEN f=θ_i,

where A_1^i and A_2^i are linguistic values of the cutting and feeding velocities of the cutter, respectively. θ_i is the fuzzy system output of rule $R^{(i)}$.

The output value of the fuzzy system is given as

$$f = \frac{\sum_{i=1}^{m}\left(\mu_{A_1^i}(\omega)\mu_{A_2^i}(v_\mathrm{f})\right)\theta_i}{\sum_{i=1}^{m}\left(\mu_{A_1^i}(\omega)\mu_{A_2^i}(v_\mathrm{f})\right)}. \tag{7}$$

Therefore, the output of the fuzzy system can be expressed as regression models:

$$f = \boldsymbol{\alpha}^\mathrm{T}\boldsymbol{\theta}, \tag{8}$$

where $\boldsymbol{\alpha}$=[α_1, α_2, …, α_m]$^\mathrm{T}$ is a regressive vector defined in Eq. (9), and $\boldsymbol{\theta}$=[θ_1, θ_2, …, θ_m]$^\mathrm{T}$ is the unknown parameter.

$$\alpha_i = \frac{\mu_{A_1^i}(\omega)\mu_{A_2^i}(v_\mathrm{f})}{\sum_{i=1}^{m}\left(\mu_{A_1^i}(\omega)\mu_{A_2^i}(v_\mathrm{f})\right)}. \tag{9}$$

Table 1 Rule base for the fuzzy logic system

ω/v_f	Z	NZ	VS	S	M	B	VB
Z	Z	Z	Z	NZ	VS	NS	S
NZ	Z	Z	NZ	VS	NS	S	NM
VS	Z	NZ	VS	NS	S	NM	M
S	NZ	VS	NS	S	NM	M	NB
M	VS	NS	S	NM	M	NB	B
B	NS	S	NM	M	NB	B	VB
VB	S	NM	M	NB	B	VB	VB

In accordance with the universal approximation theory, an optimal fuzzy system exists in the following form:

$$f = f_{\mathrm{fz}}^{*} + \varepsilon = \boldsymbol{\alpha}^{\mathrm{T}}\boldsymbol{\theta}^{*} + \varepsilon, \tag{10}$$

where ε is the approximation error and satisfies $|\varepsilon|\leq E$ (E is a positive constant). In fact, the approximated fuzzy system $\hat{f}_{\mathrm{fz}}$ is used in the controller. Therefore, the error is shown as follows:

$$\tilde{f}_{\mathrm{fz}} = f_{\mathrm{fz}}^{*} - \hat{f}_{\mathrm{fz}} = \boldsymbol{\alpha}^{\mathrm{T}}\boldsymbol{\theta}^{*} - \boldsymbol{\alpha}^{\mathrm{T}}\hat{\boldsymbol{\theta}} = \boldsymbol{\alpha}^{\mathrm{T}}\tilde{\boldsymbol{\theta}}. \tag{11}$$

A virtual controller $x_{2\mathrm{d}}$ for x_2 is shown as follows:

$$x_{2\mathrm{d}} = \frac{J}{D}\left(\dot{x}_{1\mathrm{d}} - \lambda\tilde{x}_1 - k_{11}s_1 - \frac{1}{J}\hat{E}u_{\mathrm{comp}}\right) + \frac{1}{D}\hat{f}_{\mathrm{fz}}, \tag{12}$$

where k_{11} is a positive constant, $\hat{E}$ is the bound estimation, and u_{comp} is used to compensate for the difference between the real nonlinear functions f and $\hat{f}_{\mathrm{fz}}$ and is the reaching part of sliding mode control. Here, we use a smooth signum function to obtain the twice differentiable smooth saturation u_{comp} facilitating calculation given by

$$u_{\mathrm{comp}} = 2\frac{\int_{-\Phi}^{s_1}(\tau+\Phi)^2(\Phi-\tau)^2\,\mathrm{d}\tau}{\int_{-\Phi}^{\Phi}(\tau+\Phi)^2(\Phi-\tau)^2\,\mathrm{d}\tau} - 1, \tag{13}$$

where Φ is the sliding surface boundary layer width.

Let $s_2=x_2-x_{2\mathrm{d}}$ denote the tracking error of the servo valve spool displacement. Substituting Eq. (12) into Eq. (5), we obtain the time derivative of s_1 as follows:

$$\dot{s}_1 = \frac{1}{J}(-\varepsilon - \boldsymbol{\alpha}^{\mathrm{T}}\tilde{\boldsymbol{\theta}}) - k_{11}s_1 - \frac{1}{J}\hat{E}u_{\mathrm{comp}} + \frac{D}{J}s_2. \tag{14}$$

Define $s_{1\Delta} = s_1 - \Phi\mathrm{sat}(s_1/\Phi)$ to obtain

$$\begin{cases} |s_{1\Delta}| = |s_1| - \Phi, \ \dot{s}_{1\Delta} = \dot{s}_1, \ |s_1| > \Phi, \\ s_{1\Delta} = \dot{s}_{1\Delta} = 0, \ |s_1| \leq \Phi. \end{cases} \tag{15}$$

The properties of function $s_{1\Delta}$ are used to cease adaptation when the boundary layer is reached and to avoid unbounded increase.

A Lyapunov function is defined as

$$V_1 = \frac{1}{2}s_{1\Delta}^2 + \frac{1}{2J}\frac{1}{\eta_{11}}\tilde{\boldsymbol{\theta}}^{\mathrm{T}}\tilde{\boldsymbol{\theta}} + \frac{1}{2J}\frac{1}{\eta_{12}}\tilde{E}^2, \tag{16}$$

where η_{11} and η_{12} are positive constants. The time derivative of V_1 is written as

$$\dot{V}_1 = s_{1\Delta}\dot{s}_{1\Delta} + \frac{1}{J}\frac{1}{\eta_{11}}\tilde{\boldsymbol{\theta}}^{\mathrm{T}}\dot{\tilde{\boldsymbol{\theta}}} + \frac{1}{J}\frac{1}{\eta_{12}}\tilde{E}\dot{\tilde{E}}. \tag{17}$$

Thus, if $|s_1|\leq\Phi$, then $s_{1\Delta}=0$; it follows $\dot{V}_1 = 0$. If $|s_1|>\Phi$, then $\dot{s}_{1\Delta} = \dot{s}_1$. By substituting Eq. (14) into Eq. (17) we can obtain

$$\begin{aligned} \dot{V}_1 \leq {} & -k_{11}s_1s_{1\Delta} + \frac{1}{J}\tilde{\boldsymbol{\theta}}^{\mathrm{T}}\left(s_{1\Delta}\boldsymbol{\alpha} - \frac{1}{\eta_{11}}\dot{\hat{\boldsymbol{\theta}}}\right) \\ & + \frac{1}{J}\left(|s_{1\Delta}|E - \frac{1}{\eta_{12}}\tilde{E}\dot{\hat{E}} - s_{1\Delta}\hat{E}u_{\mathrm{comp}}\right) + \frac{D}{J}s_2s_{1\Delta}. \end{aligned} \tag{18}$$

The adaptive laws are chosen as

$$\begin{cases} \dot{\hat{\boldsymbol{\theta}}} = \eta_{11}s_{1\Delta}\boldsymbol{\alpha}, \\ \dot{\hat{E}} = \eta_{12}|s_{1\Delta}|. \end{cases} \tag{19}$$

Thus, Eq. (18) can be rewritten as

$$\dot{V}_1 \leq -k_{11}s_1s_{1\Delta} + \frac{1}{J}|s_{1\Delta}|\hat{E}[1 - u_{\mathrm{comp}}\,\mathrm{sgn}(s_{1\Delta})] + \frac{D}{J}s_2s_{1\Delta}. \tag{20}$$

Step 2:

The actual control input α_{p} is determined in this step. The time derivative of s_2 can be written as

$$\dot{s}_2 = \dot{x}_2 - \dot{x}_{2\mathrm{d}} = \frac{\beta_{\mathrm{e}}}{V}(k_{\mathrm{p}}\alpha_{\mathrm{p}} - Dx_1 - c_{\mathrm{t}}x_2) - \dot{x}_{2\mathrm{d}}. \tag{21}$$

Define the Lyapunov function as

$$V_2 = V_1 + \frac{1}{2\eta_{21}}s_2^2. \tag{22}$$

Differentiate Eq. (22) with respect to time as

$$\dot{V}_2 = \dot{V}_1 + \frac{1}{\eta_{21}}s_2\dot{s}_2. \tag{23}$$

By substituting Eq. (21) into Eq. (23) we can obtain

$$\begin{aligned}\dot{V}_2 \le & \frac{1}{J}|s_{1\Delta}|\hat{E}[1-u_{\text{comp}}\,\text{sgn}(s_{1\Delta})] \\ & -k_{11}s_1 s_{1\Delta}-\frac{1}{\eta_{21}}s_2\left(\dot{x}_{2\text{d}}+\frac{D}{J}s_{1\Delta}\eta_{21}\right) \\ & +\frac{1}{\eta_{21}}s_2\frac{\beta_{\text{e}}}{V}(k_{\text{p}}\alpha_{\text{p}}-Dx_1-c_{\text{t}}x_2).\end{aligned} \tag{24}$$

Then the control law can be expressed as

$$\begin{aligned}\alpha_{\text{p}} = & \frac{1}{k_{\text{p}}}(Dx_1+c_{\text{t}}x_2) \\ & +\frac{1}{k_{\text{p}}}\frac{V}{\beta_{\text{e}}}\left(-k_{21}s_2+\dot{x}_{2\text{d}}+\frac{D}{J}s_{1\Delta}\eta_{21}\right).\end{aligned} \tag{25}$$

Thus, Eq. (24) can be rewritten as

$$\begin{aligned}\dot{V}_2 \le & -k_{11}s_1 s_{1\Delta}-\frac{1}{\eta_{21}}k_{21}s_2^2, \\ & +\frac{1}{J}|s_{1\Delta}|\hat{E}[1-u_{\text{comp}}\,\text{sgn}(s_{1\Delta})].\end{aligned} \tag{26}$$

Therefore, if $|s_1|\le\Phi$, then $s_{1\Delta}=0$ and $\dot{V}_2<0$. Else if $|s_1|>\Phi$, then $s_1 s_{1\Delta}>0$ and $1-u_{\text{comp}}\,\text{sgn}(s_{1\Delta})=0$; it follows $\dot{V}_2<0$.

The stability of the overall closed-loop system, consisting of the controller and the adaptive fuzzy system, is guaranteed, and all the signals involved in the system are proved to be bounded. Fig. 3 shows the block diagram of the whole system.

4 Experimental verification

4.1 Test bench setup

In this section, we describe the experiments carried out to verify the effectiveness of the proposed controller. The experimental installation is presented in Fig. 4 and the structure of the test rig in Fig. 5. In general, the experimental equipment contains mainly the cutting velocity control system (CVCS) and the load generating system (LGS). A variable displacement axial piston pump with an external pilot oil supply was driven by a three-phase asynchronous motor which rotates at a constant speed of 1450 r/min. The displacement control of the pump was accomplished by means of a pilot servo valve with electrical feedback of the swashplate angle. Through a swashplate angle feedback, the current signal to the pilot servo valve determines the swashplate angle via the control piston and thus the pump displacement. The other servo valve controlled loading motor was used to simulate a load acting on the cutting motor and

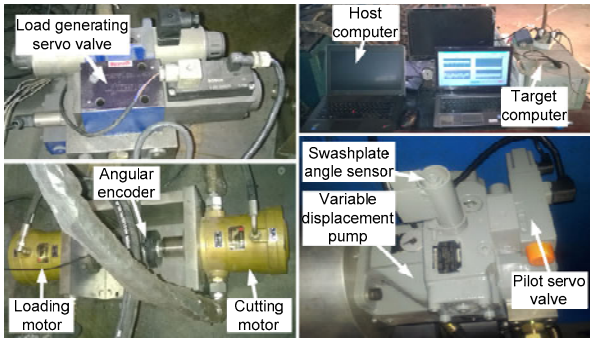

Fig. 4 Experimental test rig

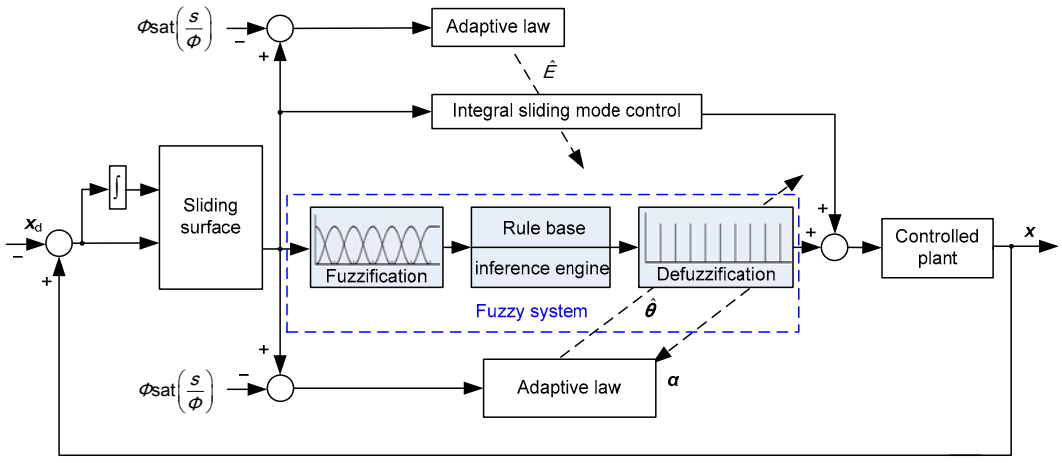

Fig. 3 Structure of the AFISMC for cutting velocity control

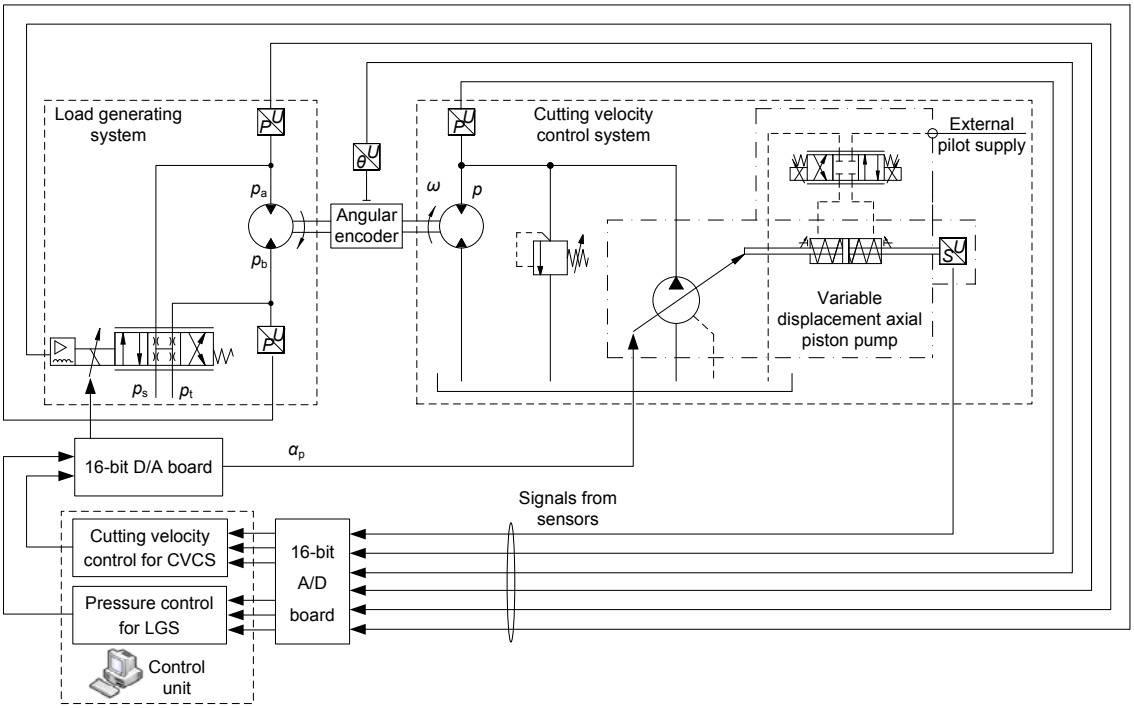

Fig. 5 Structure of the test rig

generating pressure disturbance in the motor velocity control process. The pressures of the test system were measured by pressure sensors and the angular velocity of the hydraulic motors was obtained by differentiating the angular signal which was measured by the angle encoder. A compatible PC including a 16-bit multifunction data acquisition and control card was used to acquire the sensor signals and generate control signals to the variable displacement pump and the load generating servo valve. The cutting velocity controller and the load generating controller were both implemented in the MATLAB/xPC target environment and the sampling time was 1 ms.

4.2 Experimental results

First, we focus on the ability of the proposed controller to overcome disturbances in the control of velocity in the cutting system in four different geological conditions: soil, hard soil, limestone, and granite. To evaluate the control performance of AFISMC in the cutting system, we used a constant velocity reference (1500 r/min) with load disturbances introduced through the feeding velocity of the cutter. The flow rate disturbance signal through the feeding motor was a sinusoidal signal with an amplitude of 5 L/min and a frequency of 0.25 Hz.

Three control algorithms were compared in the experiments and first tested in soil. The first was the conventional PI controller. The PI gains were tuned by trial and error, and the determined PI gains proved to be better than those of the other algorithms in this operating condition. The PI controller used in the experiments is expressed as follows:

$$u = 2\times10^{-3}(x_{1\mathrm{d}} - x_1) + 4.5\times10^{-2}\int_0^t (x_{1\mathrm{d}} - x_1)\mathrm{d}t. \quad (27)$$

The second was an integral sliding mode controller (ISMC) without fuzzy approximation. A smooth signum function was used to reduce the chattering phenomenon of the ISMC control law. The ISMC controller can be expressed as

$$\begin{cases} x_{2\mathrm{d}} = \dfrac{J}{D}\left(\dot{x}_{1\mathrm{d}} - \lambda\tilde{x}_1 - k_{11}s_1 - \dfrac{1}{J}\hat{E}u_{\mathrm{comp}}\right), \\ \alpha_{\mathrm{p}} = \dfrac{1}{k_{\mathrm{p}}}(Dx_1 + c_{\mathrm{t}}x_2) \\ \qquad + \dfrac{1}{k_{\mathrm{p}}}\dfrac{V}{\beta_{\mathrm{e}}}\left(-k_{21}s_2 + \dot{x}_{2\mathrm{d}} + \dfrac{D}{J}s_{1\Delta}\eta_{21}\right). \end{cases} \quad (28)$$

The third algorithm was the proposed AFISMC. The unknown bound of the disturbance increases the complexity of the calculation of the feedback gain of the reaching controller to ensure theoretical rigor. An alternative pragmatic approach is simply to choose a large enough feedback gain without worrying about specific prerequisites. This approach increases the tuning efficiency. The fuzzy system parameters were selected according to engineering experience and the control gains were tuned by trial and error based on the desired dynamic response. The boundary layer thickness (Φ) was selected on the basis of a compromise between the chattering phenomenon and the tracking accuracy. The proposed AFISMC parameters are shown in Table 2.

Table 2 AFISMC control parameters

Parameter	Value	Parameter	Value
λ	20	η_{11}	20
k_{11}	500	η_{12}	10^{-6}
k_{21}	100	η_{21}	10^{-6}
Φ	0.5		

The corresponding tracking errors of AFISMC, ISMC, and PI with disturbances in soil are shown in Fig. 6. The three controllers showed similar control performance and the tracking errors were less than 20 r/min in the experiment. Therefore, the three controllers all obtained satisfactory control performance with external disturbances in soil.

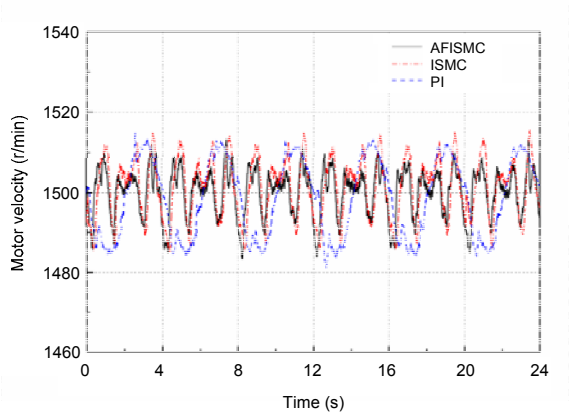

Fig. 6 Constant tracking with disturbance in soil

Load torque acting on the cutting motor in soil using AFISMC is shown in Fig. 7. The load torque was calculated from the pressure difference and displacement of the load generating motor. Although the desired cutting velocity of the cutter is constant, the load torque acting on the motor varies with its feeding velocity because of the particular characteristics of the cutting system.

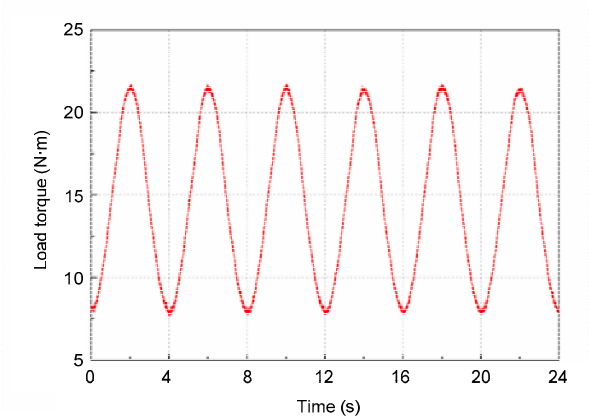

Fig. 7 Load torque acting on the cutting motor in soil using AFISMC

The swashplate angle of the pump in this operating condition using AFISMC is shown in Fig. 8, and the corresponding transient inlet pressure of the cutting motor in Fig. 9. They are both bounded as assumed.

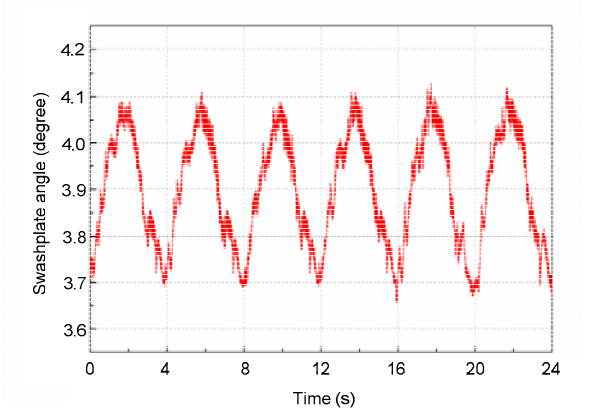

Fig. 8 Swashplate angle of the pump in soil using AFISMC

To further test the performance of AFISMC, we changed the geological condition to hard soil. The corresponding tracking errors of AFISMC, ISMC, and PI with disturbances in hard soil are shown in Fig. 10. The three controllers showed similar control performance and the errors were all nearly 20 r/min

during the falling process of the disturbance signal. However, the AFISMC achieved a superior control performance than the other two controllers during the rising process in the experiment when confronted with a harder operating condition, which demonstrates the effectiveness of the proposed controller.

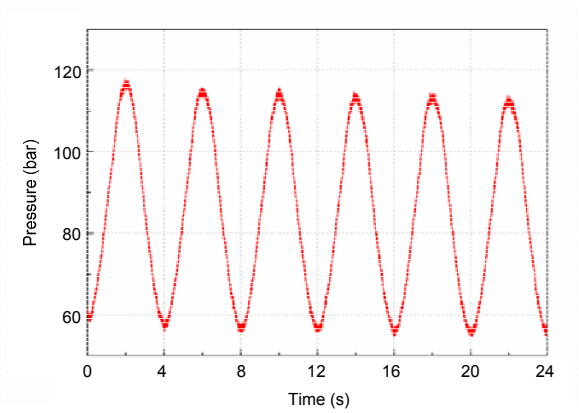

Fig. 9 The transient inlet pressure of cutting motor in soil using AFISMC

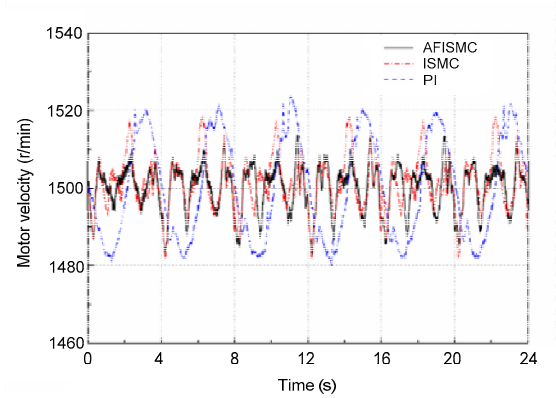

Fig. 10 Constant tracking with disturbance in hard soil

The tracking errors of the three controllers with disturbances in limestone and granite are shown in Figs. 11 and 12, respectively. The PI and ISMC controllers showed large control errors. In contrast, the proposed controller always had better robustness than the PI and ISMC controllers in these two operating conditions. This indicates that the proposed controller can effectively overcome external disturbances in different operating conditions.

As previously stated, the conventional PI controller and the ISMC controller could achieve relatively good control performance similar to that of the proposed controller in soil and even in hard soil. However, they showed poor performance in limestone and granite and thus cannot cover all the operating conditions. This occurs because the PI controller is not robust enough with respect to the varying operating conditions and the ISMC controller has only a certain amount of robustness without an adaptive fuzzy system which can compensate for the unmodeled disturbances of the cutting system. In contrast, the proposed controller shows consistent control performance. The desired motor velocity is well tracked by the proposed AFISMC controller with feeding velocity disturbance under various operating conditions demonstrating its robustness.

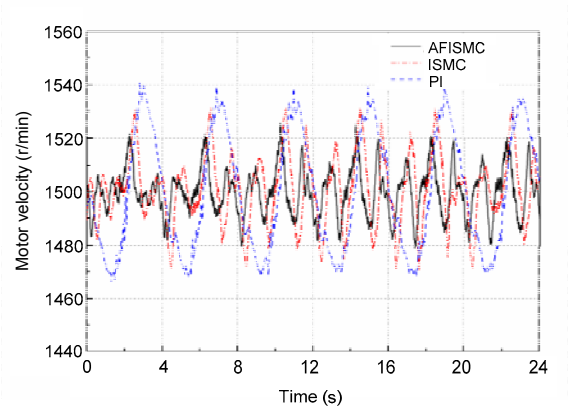

Fig. 11 Constant tracking with disturbance in limestone

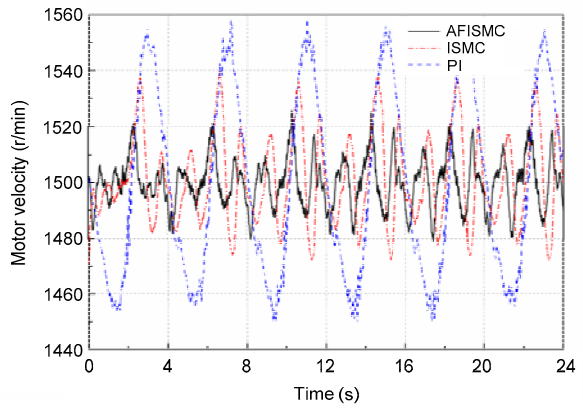

Fig. 12 Constant tracking with disturbance in granite

Finally, to evaluate the control of tracking performance of AFISMC for the cutting system, we used a sinusoidal velocity reference with a constant feeding velocity. The desired velocity tracking trajectory was a sinusoidal signal with an amplitude of 1000 r/min and a frequency of 0.25 Hz.

Fig. 13 shows the sinusoidal velocity tracking results of the three controllers in soil. The maximum tracking errors of the PI and ISMC controllers were respectively about 50 r/min and 35 r/min and there was a certain phase lag. The tracking error of the proposed AFISMC controller was always less than 20 r/min. The AFISMC obviously exhibits better performance in soil than the PI and ISMC controllers in terms of the transient tracking error.

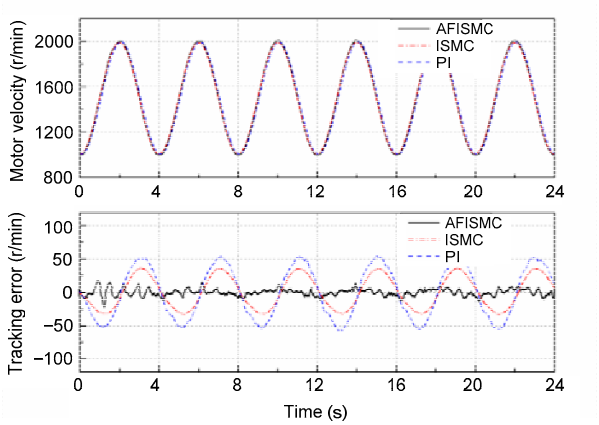

Fig. 13 Sinusoidal tracking of the system in soil

Fig. 14 shows the sinusoidal velocity tracking results of the three controllers in hard soil. When confronted with a harder operating condition, AFISMC still achieved a superior tracking performance in comparison with PI and ISMC controllers, demonstrating the effectiveness of AFISMC.

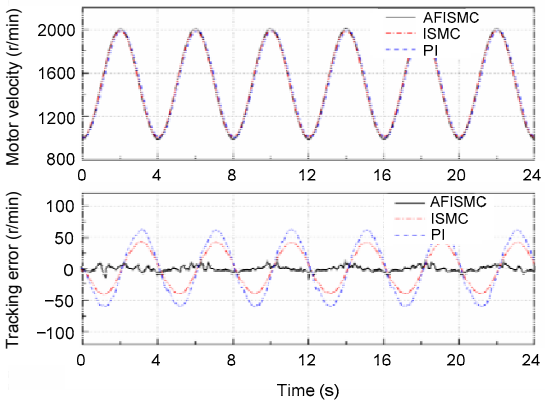

Fig. 14 Sinusoidal tracking of the system in hard soil

Fig. 15 shows the sinusoidal velocity tracking results of the three controllers in limestone. The maximum transient tracking error of the PI controller was about 80 r/min and the maximum error of the ISMC reached 50 r/min. In contrast, the proposed controller showed a tracking performance consistent with the previous experiments. This indicates that the proposed controller can achieve high tracking accuracy and fast response under various operating conditions.

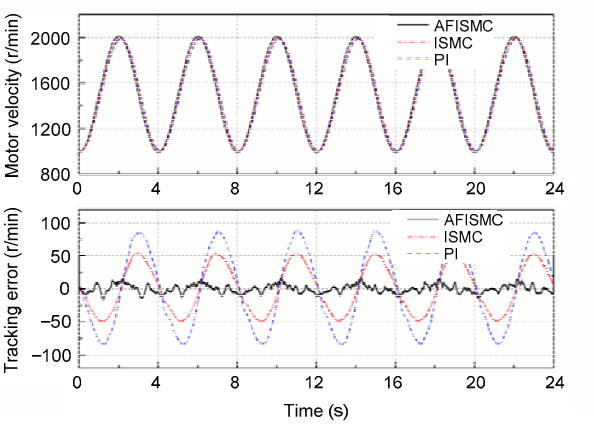

Fig. 15 Sinusoidal tracking of the system in limestone

Fig. 16 shows the sinusoidal velocity tracking experimental results of the three controllers in granite. The AFISMC showed its advantage in comparison with PI and ISMC controllers. The maximum tracking error of the proposed controller was about 50 r/min at the beginning of the experiment. However, as the experiment continued, the proposed control scheme showed higher tracking accuracy. The tracking error of the AFISMC controller achieved a rapid asymptotic decrease in the process of the approximation error of adaptive fuzzy system convergence through

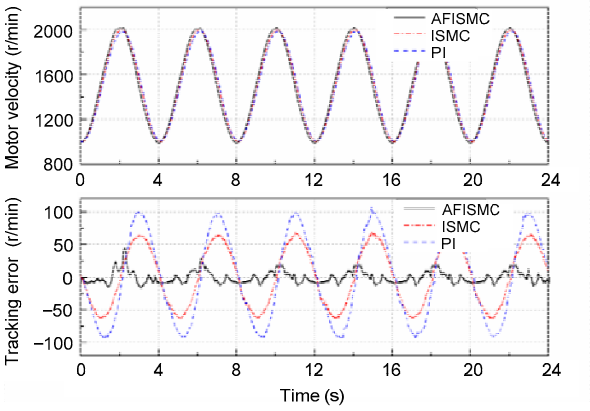

Fig. 16 Sinusoidal tracking of the system in granite

the fuzzy parameters tuning online and finally converged to less than 25 r/min. Therefore, the adaptive fuzzy system can decrease the tracking error through the adaptive law for the fuzzy system.

In summary, the AFISMC achieved a good tracking performance with a higher tracking accuracy and faster response than PI and ISMC controllers in all four different operating conditions, which shows the effectiveness of the proposed controller in terms of transient tracking errors.

5 Conclusions

In this study, the control of the cutting velocity of a cutting system was explored. To deal with the particular characteristics of a cutting system, an AFISMC scheme was designed to control the cutting velocity. The proposed controller combines the robust characteristics of an integral sliding mode controller and the adaptive adjusting characteristics of an adaptive fuzzy controller. The AFISMC cutting velocity controller was synthesized using a backstepping technique. The stability of the whole system, including the integral sliding mode controller, adaptive fuzzy system, and the controlled plant, was proven using the Lyapunov theory. Finally, the effectiveness of the proposed controller was verified by experimental results.

References

Ahn, K.K., Chau, N.H.T., Truong, D.Q., 2007. Robust force control of a hybrid actuator using quantitative feedback theory. *J. Mech. Sci. Technol.*, **21**(12):2048-2058. http://dx.doi.org/10.1007/BF03177463

Busquets, E., Ivantysynova, M., 2015. Discontinuous projection-based adaptive robust control for displacement-controlled actuators. *J. Dyn. Syst. Meas. Contr.*, **137**(8): 081007. http://dx.doi.org/10.1115/1.4030064

Cerman, O., 2013. Fuzzy model reference control with adaptation mechanism. *Expert Syst. Appl.*, **40**(13):5181-5187. http://dx.doi.org/10.1016/j.eswa.2013.03.014

Chen, C.Y., Liu, L.Q., Cheng, C.C., *et al*., 2008. Fuzzy controller design for synchronous motion in a dual-cylinder electro-hydraulic system. *Contr. Eng. Pract.*, **16**(6): 658-673. http://dx.doi.org/10.1016/j.conengprac.2007.08.005

Chiang, M.H., Lee, L.W., Tsai, J.J., 2004. The concurrent implementation of high velocity control performance and high energy efficiency for hydraulic injection moulding machines. *Int. J. Adv. Manuf. Technol.*, **23**(3):256-262. http://dx.doi.org/10.1007/s00170-003-1652-8

Chiang, M.H., Yeh, Y.P., Yang, F.L., *et al.*, 2005. Integrated control of clamping force and energy-saving in hydraulic injection moulding machines using decoupling fuzzy sliding-mode control. *Int. J. Adv. Manuf. Technol.*, **27**(1):53-62. http://dx.doi.org/10.1007/s00170-004-2138-z

Daher, N., Ivantysynova, M., 2013. System synthesis and controller design of a novel pump controlled steer-by-wire system employing modern control techniques. Proc. ASME/BATH Symp. on Fluid Power and Motion Control, p.1-10. http://dx.doi.org/10.1115/FPMC2013-4410

Daher, N., Ivantysynova, M., 2014. An indirect adaptive velocity controller for a novel steer-by-wire system. *J. Dyn. Syst. Meas. Contr.*, **136**(5):051012. http://dx.doi.org/10.1115/1.4027172

Guo, K., Wei, J.H., Fang, J.H., *et al.*, 2015. Position tracking control of electro-hydraulic single-rod actuator based on an extended disturbance observer. *Mechatronics*, **27**: 47-56. http://dx.doi.org/10.1016/j.mechatronics.2015.02.003

Kalyoncu, M., Haydim, M., 2009. Mathematical modelling and fuzzy logic based position control of an electrohydraulic servosystem with internal leakage. *Mechatronics*, **19**(6):847-858. http://dx.doi.org/10.1016/j.mechatronics.2009.04.010

Lin, J., Huang, Z.Z., 2007. A hierarchical fuzzy approach to supervisory control of robot manipulators with oscillatory bases. *Mechatronics*, **17**(10):589-600. http://dx.doi.org/10.1016/j.mechatronics.2007.07.008

Lin, Y., Shi, Y., Burton, R., 2013. Modeling and robust discrete-time sliding-mode control design for a fluid power electrohydraulic actuator (EHA) system. *IEEE/ASME Trans. Mech.*, **18**(1):1-10. http://dx.doi.org/10.1109/TMECH.2011.2160959

Merritt, H.E., 1967. Hydraulic Control Systems. John Wiley & Sons, New York, USA.

Minav, T.A., Laurila, L.I.E., Pyrhönen, J.J., 2013. Analysis of electro-hydraulic lifting system's energy efficiency with direct electric drive pump control. *Autom. Constr.*, **30**:144-150. http://dx.doi.org/10.1016/j.autcon.2012.11.009

Sha, D.H., Bajic, V.B., Yang, H.Y., 2002. New model and sliding mode control of hydraulic elevator velocity tracking system. *Simul. Practice Theory*, **9**(6-8):365-385. http://dx.doi.org/10.1016/S1569-190X(02)00058-8

Shi, Y., Huang, J., Yu, B., 2013. Robust tracking control of networked control systems: application to a networked DC motor. *IEEE Trans. Ind. Electron.*, **60**(12):5864-5874. http://dx.doi.org/10.1109/TIE.2012.2233692

Truong, D.Q., Ahn, K.K., 2009. Force control for hydraulic load simulator using self-tuning grey predictor—fuzzy PID. *Mechatronics*, **19**(2):233-246. http://dx.doi.org/10.1016/j.mechatronics.2008.07.007

Truong, D.Q., Ahn, K.K., 2011. Force control for press machines using an online smart tuning fuzzy PID based on a

robust extended Kalman filter. *Expert Syst. Appl.*, **38**(5): 5879-5894. http://dx.doi.org/10.1016/j.eswa.2010.11.035

Wang, D.Y., Lin, X., Zhang, Y., 2011. Fuzzy logic control for a parallel hybrid hydraulic excavator using genetic algorithm. *Autom. Constr.*, **20**(5):581-587. http://dx.doi.org/10.1016/j.autcon.2010.11.024

Wang, L.K., Book, W.J., Huggins, J.D., 2012. Application of singular perturbation theory to hydraulic pump controlled systems. *IEEE/ASME Trans. Mech.*, **17**(2):251-259. http://dx.doi.org/10.1109/TMECH.2010.2096230

Wang, X.J., Wang, S.P., Zhao, P., 2012. Adaptive fuzzy torque control of passive torque servo systems based on small gain theorem and input-to-state stability. *Chin. J. Aeronaut.*, **25**(6):906-916. http://dx.doi.org/10.1016/S1000-9361(11)60461-5

Wei, J.H., Guo, K., Fang, J.H., *et al.*, 2015. Nonlinear supply pressure control for a variable displacement axial piston pump. *Proc. Inst. Mech. Eng. Part I: J. Syst. Contr. Eng.*, **229**(7):614-624. http://dx.doi.org/10.1177/0959651815577546

Wei, L., Fang, F., Shi, Y., 2014. Adaptive backstepping-based composite nonlinear feedback water level control for the nuclear U-tube steam generator. *IEEE Trans. Contr. Syst. Technol.*, **22**(1):369-377. http://dx.doi.org/10.1109/TCST.2013.2250504

Wu, H.W., Lee, C.B., 1995. Self-tuning adaptive speed control of a pump/inverter-controlled hydraulic motor system. *Proc. Inst. Mech. Eng. Part I: J. Syst. Contr. Eng.*, **209**(29):101-114. http://dx.doi.org/10.1243/PIME-PROC-1995-209-37

Zhang, H., Shi, Y., Mu, B.X., 2013. Optimal H_∞-based linear-quadratic regulator tracking control for discrete-time Takagi-Sugeno fuzzy systems with preview actions. *J. Dyn. Syst. Meas. Contr.*, **135**(4):044501. http://dx.doi.org/10.1115/1.4024007